

THEORY OF COSMIC MICROWAVE BACKGROUND POLARIZATION*

PAOLO CABELLA[†]

Dipartimento di Fisica, Università Tor Vergata, Roma I-00133, Italy

MARC KAMIONKOWSKI[‡]

California Institute of Technology, Mail Code 130-33, Pasadena, CA 91125, USA

These lectures introduce some of the basic theory of cosmic microwave background (CMB) polarization with the primary aim of developing the theory of CMB polarization from inflationary gravitational waves, as well as some of the related theory of weak gravitational lensing (cosmic shear) of CMB polarization. We begin with production of polarization by Thomson scattering. We then discuss tensor-harmonic analysis (the “grad-curl” or “E-B” decomposition) on a flat and full sky in some detail. The Boltzmann/Einstein equations required to predict the CMB temperature/polarization pattern due to primordial gravitational waves are derived. We show that gravitational waves produce a curl component of the CMB polarization while density perturbations (at linear order) do not. We then show how cosmic shear induces a curl component from a curl-free surface of last scattering. We describe, though in less detail, how higher-order correlations can be used to subtract the cosmic-shear-induced curl. Several exercises are provided.

1. Introduction

Just five years ago, the small-scale structure of the CMB was hidden behind a veil of experimental limitation. That is no longer the case. We now know empirically that the CMB has a wealth of detailed information in its temperature [1] and polarization pattern [2]. We are now also confident in our theoretical understanding of these fluctuations: they are produced by a nearly scale-invariant spectrum of primordial density perturbations. With a solid theoretical foundation, we are poised to move considerably further with future more precise CMB experiments. Prospects for new advances include an even more detailed picture of the physics at the surface of last scattering, the physics of inflation, gravitational-wave backgrounds, the distribution of mass in the intermediate-redshift and current Universe, and perhaps the behavior of the dark energy.

*Lectures given at the 2003 Villa Mondragone School of Gravitation and Cosmology: “The Polarization of the Cosmic Microwave Background,” Rome, Italy, September 6–11, 2003.

[†]Paolo.Cabella@roma2.infn.it

[‡]kamion@tapir.caltech.edu

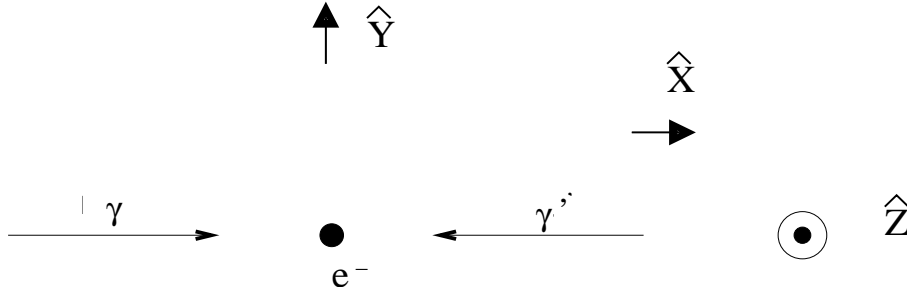


Fig. 1. Radiation incident on an electron from the $\pm\hat{x}$ directions scatters into the \hat{z} direction by shaking the electron in the $\pm\hat{y}$ direction.

These lectures will *not* discuss all these wonderful possibilities. Instead, we focus here on detailing some of the basics of the theory of CMB polarization with the aim primarily of understanding the polarization due to inflationary gravitational waves, as well as the related effects of weak gravitational lensing (“cosmic shear”) on CMB polarization. There is now a vast literature on CMB theory, including a number of reviews [3] and even a few books [4]. Thus, experts are unlikely to find anything new in here. However, some students may find that the discussion and level of detail for the specific subjects on which we focus provide a useful complement to these other more comprehensive sources. In particular, we discuss tensor harmonics (the “curl-grad” or “E-B” decomposition) on both a flat and a full sky in detail, and we provide a detailed justification, from scratch, of the statement that gravitational waves produce a curl component in the CMB while density perturbations do not. We show in detail that cosmic shear induces a curl component in the CMB polarization, but our discussion of how this shear may be subtracted with higher-order correlations is a bit sketchier. We do not deal with any of the many important issues in data analysis.

The plan of the lectures is as follows: We begin in Section 2 by reviewing how Thomson scattering produces polarization. Section 3 develops tensor harmonic analysis on a flat sky and Section 4 deals briefly with flat-sky correlation functions. Section 5 deals with tensor harmonic analysis on the full sky and Section 6 with the correlation functions. Section 7 provides some comments, and in Section 8 we discuss some of the effects of cosmic shear on the polarization pattern. A few exercises are sprinkled throughout to help conscientious students develop their facility with subject matter. We reference primarily the most important original papers on relevant subjects and/or those that were particularly useful to us in the preparation of these lectures, but our referencing does not provide a full guide to the literature. For that we refer the reader to the more comprehensive reviews [3].

2. Polarization of CMB: Theory

Let us begin by understanding in the most basic terms why the CMB should be

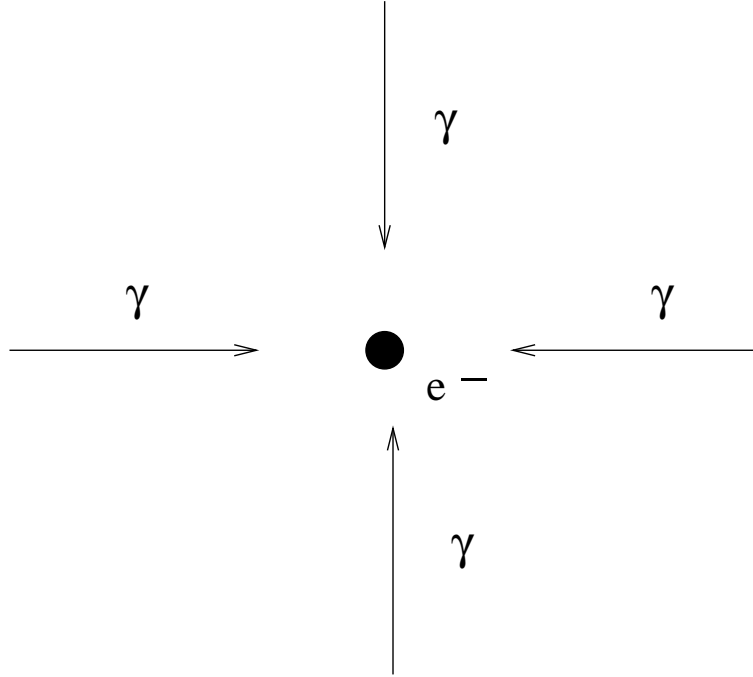


Fig. 2. Radiation incident on the electron with equal intensities in the $\pm\hat{x}$ and $\pm\hat{y}$ directions will be unpolarized when scattered to the \hat{z} direction.

polarized [5]. Consider scattering of an electromagnetic wave propagating in the $\pm\hat{x}$ direction in the plane of the page that then scatters to the observer (perpendicular to the page) by 90° ; the scatterer is a free electron (Fig. 1). If the incident radiation is linearly polarized with an \vec{E} vector in the \hat{z} direction, then the electron oscillates in the \hat{z} direction and emits no dipole radiation toward the observer. But if the incident radiation is polarized in the \hat{y} direction, the electron oscillates in the \hat{y} direction and the dipole radiation the observer sees is linearly polarized in the $\pm\hat{y}$ direction. If the incident radiation is unpolarized then only the component with $\vec{E} \parallel \hat{y}$ is scattered toward the observer, and the resulting scattered radiation is polarized in the \hat{y} direction. Likewise if the incident radiation comes only from the $\pm\hat{y}$ direction, then the observed scattered radiation will be polarized in the $\pm\hat{x}$ direction.

Now if we have radiation incident from the $\pm\hat{x}$ and $\pm\hat{y}$ directions with equal intensities (see Fig. 2), then the polarizations in the $\pm\hat{x}$ and $\pm\hat{y}$ directions will cancel, and the scattered radiation will be unpolarized. But if the intensity in the \hat{x} direction slightly exceeds that in the \hat{y} direction, then the scattered radiation will be slightly polarized in the \hat{y} direction.

To proceed further we must now introduce the Stokes parameters Q and U for linear polarization. Most generally, a monochromatic electromagnetic wave propa-

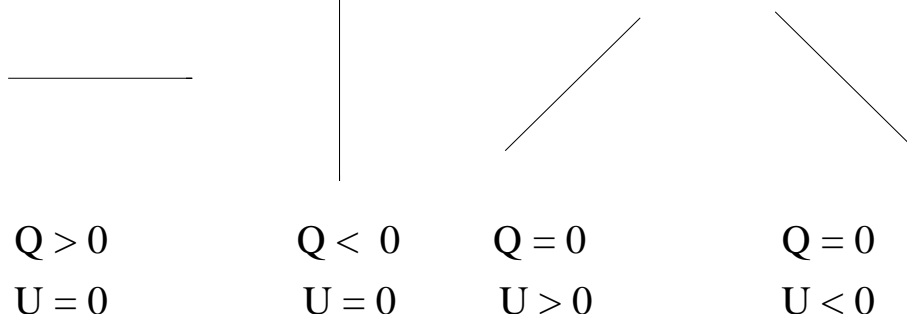


Fig. 3. The linear-polarization states described various combinations of Stokes parameters Q and U .

gating in the \hat{z} direction has an electric-field vector,

$$E_x = a_x \cos(\omega t - \xi_x); \quad E_y = a_y \cos(\omega t - \xi_y). \quad (1)$$

The Stokes parameters are then the intensity,

$$I = a_x^2 + a_y^2, \quad (2)$$

linear-polarization parameters,

$$Q = a_x^2 - a_y^2, \quad U = 2a_x a_y \cos(\xi_x - \xi_y), \quad (3)$$

and circular-polarization parameter,

$$V = 2a_x a_y \sin(\xi_x - \xi_y). \quad (4)$$

The last Stokes parameter V vanishes as Thomson scattering induces no circular polarization (but see Ref. [8]). The parameter Q quantifies the polarization in the x - y directions while U quantifies it along axes rotated by 45° . Fig. 3 illustrates the linear polarization described by various combinations of Q and U .

If we rotate the x - y axes by an angle α about the line of sight \hat{z} , then the new x' - y' coordinates are

$$\begin{pmatrix} x' \\ y' \end{pmatrix} = \begin{pmatrix} \cos \alpha & \sin \alpha \\ -\sin \alpha & \cos \alpha \end{pmatrix} \begin{pmatrix} x \\ y \end{pmatrix}, \quad (5)$$

but the Stokes parameters (Q, U) transform as [9]

$$\begin{pmatrix} Q' \\ U' \end{pmatrix} = \begin{pmatrix} \cos 2\alpha & \sin 2\alpha \\ -\sin 2\alpha & \cos 2\alpha \end{pmatrix} \begin{pmatrix} Q \\ U \end{pmatrix}. \quad (6)$$

Formally, (Q, U) are two quantities that under a coordinate transformation,

$$x'_i = A_i^k x_k, \quad (7)$$

transform as

$$P'_{ij} = A_i^k A_j^l P_{kl}. \quad (8)$$

More explicitly, (Q, U) are the components of a symmetric trace-free 2×2 tensor,

$$\begin{pmatrix} Q & U \\ U & -Q \end{pmatrix} \Rightarrow \begin{pmatrix} \cos \alpha & \sin \alpha \\ -\sin \alpha & \cos \alpha \end{pmatrix} \begin{pmatrix} Q & U \\ U & -Q \end{pmatrix} \begin{pmatrix} \cos \alpha & -\sin \alpha \\ \sin \alpha & \cos \alpha \end{pmatrix}, \quad (9)$$

or alternatively and equivalently, a spin-2 field.

We now return to the generation of polarization by Thomson scattering. Generalizing our earlier heuristic results, the magnitude of the polarization of the scattered radiation is proportional to the magnitude of the quadrupole of the radiation incident on the scattering electron, and the orientation of the polarization is determined by the orientation of the quadrupole. More precisely, from the angular dependence [6],

$$\frac{d\sigma}{d\Omega} = \frac{3\sigma_T}{8\pi} |\hat{\epsilon}' \cdot \hat{\epsilon}|^2, \quad (10)$$

of Thomson scattering, where σ_T is the Thomson cross section and $\hat{\epsilon}'$ and $\hat{\epsilon}$ are the polarization of the incident and scattered radiation, respectively, it can be shown that the polarization of radiation scattered from an electron cloud of optical depth $\tau \ll 1$ into the \hat{z} direction is

$$Q - iU = \sqrt{\frac{3}{40\pi}} \tau a_{22}. \quad (11)$$

Here, a_{22} is the radiation quadrupole moment incident on the electron cloud. More precisely, a_{22} is the coefficient of the spherical harmonic $Y_{22}(\theta, \phi)$ in a spherical-harmonic expansion of the incident-radiation intensity in a coordinate system in which the line of sight is the \hat{z} direction, \hat{x} and \hat{z} are in the scattering plane, and Q and U are measured with respect to the x and y axes. (See Ref. [7] for expressions for more general orientations.)

Exercise 1. Verify Eq. (11).

Finally (!) we can see why the CMB must be polarized. We see angular variations in the temperature of the CMB implying temperature (and thus intensity) inhomogeneities at the CMB surface of last scattering. Thus, most generally, a given scatterer at the last-scattering surface will see an anisotropic distribution of incident radiation leading to polarized scattered radiation. For example, the radiation in the center of Fig. 4 will be polarized in the direction of the two cold spots in the temperature field.

3. Harmonic analysis for Q and U on a flat sky

According to inflation (as well as other structure-formation theories), the temperature pattern on the sky is a single realization of a random field. The simplest (and for a Gaussian field only non-trivial) statistic to describe the temperature pattern is the power spectrum C_l^{TT} .

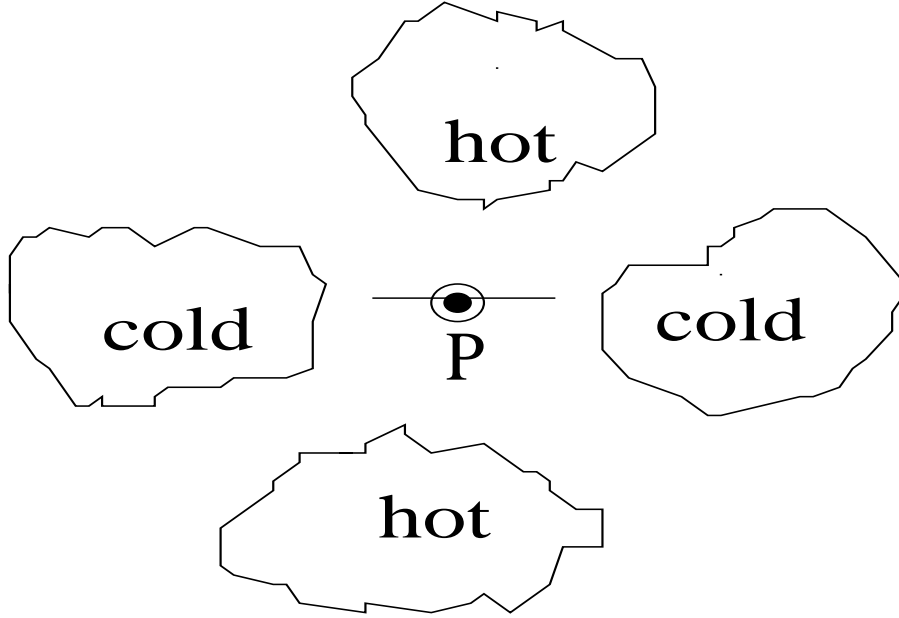


Fig. 4. The radiation scattered from the center of this quadrupolar temperature pattern will be polarized as shown.

Suppose that we now have in addition to the temperature pattern the polarization, quantified by Stokes parameters $Q(\hat{n})$ and $U(\hat{n})$ measured as a function of position $\hat{n} = (\theta, \phi)$ on the sky. Again, since Q and U are components of a symmetric trace-free (STF) 2×2 tensor, they depend on the coordinate system we choose. To discuss physics, we will thus want to find a coordinate-system-independent representation of this tensor field. Later, we will need to do this on the full sky, but as a warmup, we will first do the simpler case of a flat sky (which also serves as a good approximation to a small region of the sky).

Before moving further, it should be noted that the formalism we are about to develop also applies to cosmic-shear (weak gravitational lensing) maps, where the ellipticity parameters ϵ_+ and ϵ_\times are, like Q and U , components of a STF 2×2 tensor [10].

Once we have measured the polarization, $Q(\vec{\theta})$ and $U(\vec{\theta})$, as a function of position $\vec{\theta} = (\theta_x, \theta_y)$ on a flat region of sky, we have measured the polarization tensor field,

$$P_{ab} = \frac{1}{2} \begin{pmatrix} Q(\vec{\theta}) & U(\vec{\theta}) \\ U(\vec{\theta}) & -Q(\vec{\theta}) \end{pmatrix}, \quad (12)$$

which is sometimes written as a vector, $P_a(Q, U) = P(Q, U)$, although this is a dangerous thing to do as Q and U do not transform as the components of a vector. The polarization is also sometimes written as a complex number,

$$P = |P|e^{2i\alpha} = (Q^2 + U^2)^{1/2}e^{2i\alpha} = Q + iU, \quad (13)$$

where $|P| = (Q^2 + U^2)^{1/2}$ is the magnitude of the polarization and $\alpha = (1/2) \arctan(U/Q)$ is its orientation relative to the x axis.

We now define gradient ('G', also known as E) and curl ('C', also known as B) components of the tensor field that are independent of the orientation of the x - y axes as follows:

$$\nabla^2 P_G = \partial_a \partial_b P_{ab} \quad ; \quad \nabla^2 P_C = \epsilon_{ac} \partial_a \partial_c P_{ab}, \quad (14)$$

where ϵ_{ab} is the antisymmetric tensor.

We can write more explicit expressions for these G and C components in Fourier space. Writing

$$P_{ab}(\vec{\theta}) = \int \frac{d^2 \vec{l}}{(2\pi)^2} \tilde{P}_{ab}(\vec{l}) e^{-i\vec{l} \cdot \vec{\theta}}, \quad (15)$$

$$\tilde{P}_{ab}(\vec{l}) = \int d^2 \vec{\theta} P_{ab}(\vec{\theta}) e^{i\vec{l} \cdot \vec{\theta}}, \quad (16)$$

the Fourier components of $P_G(\vec{\theta})$ and $P_C(\vec{\theta})$ are

$$\tilde{P}_G(\vec{l}) = \frac{1}{2} \frac{(l_x^2 - l_y^2) \tilde{Q}(\vec{l}) + 2l_x l_y \tilde{U}(\vec{l})}{l_x^2 + l_y^2}, \quad (17)$$

$$\tilde{P}_C(\vec{l}) = \frac{1}{2} \frac{2l_x l_y \tilde{Q}(\vec{l}) - (l_x^2 - l_y^2) \tilde{U}(\vec{l})}{l_x^2 + l_y^2}. \quad (18)$$

Exercise 2. Verify these expressions for the Fourier components \tilde{P}_G and \tilde{P}_C , and verify that they are invariant under a rotation of the $\theta_x - \theta_y$ axes.

For a temperature map $T(\vec{\theta})$, the temperature power spectrum C_l^{TT} is defined from

$$\langle \tilde{T}(\vec{l}) \tilde{T}(\vec{l}') \rangle = (2\pi)^2 \delta(\vec{l} + \vec{l}') C_l^{\text{TT}}, \quad (19)$$

where the angle brackets denote an average over all realizations. Likewise, the statistics of the polarization field are determined by polarization power spectra C_l^{GG} , C_l^{CC} , and C_l^{GC} defined by

$$\langle \tilde{P}_G(\vec{l}) \tilde{P}_G(\vec{l}') \rangle = (2\pi)^2 \delta(\vec{l} + \vec{l}') C_l^{\text{GG}}, \quad (20)$$

$$\langle \tilde{P}_C(\vec{l}) \tilde{P}_C(\vec{l}') \rangle = (2\pi)^2 \delta(\vec{l} + \vec{l}') C_l^{\text{CC}}, \quad (21)$$

$$\langle \tilde{P}_G(\vec{l}) \tilde{P}_C(\vec{l}') \rangle = (2\pi)^2 \delta(\vec{l} + \vec{l}') C_l^{\text{GC}}. \quad (22)$$

If we also consider cross-correlation of the polarization with temperature, then there are in total six power spectra,

$$\langle \tilde{X}_1(\vec{l}) \tilde{X}_2(\vec{l}') \rangle = (2\pi)^2 \delta(\vec{l} + \vec{l}') C_l^{X_1 X_2}, \quad (23)$$

where $X_1, X_2 = \{T, P_G, P_C\}$.

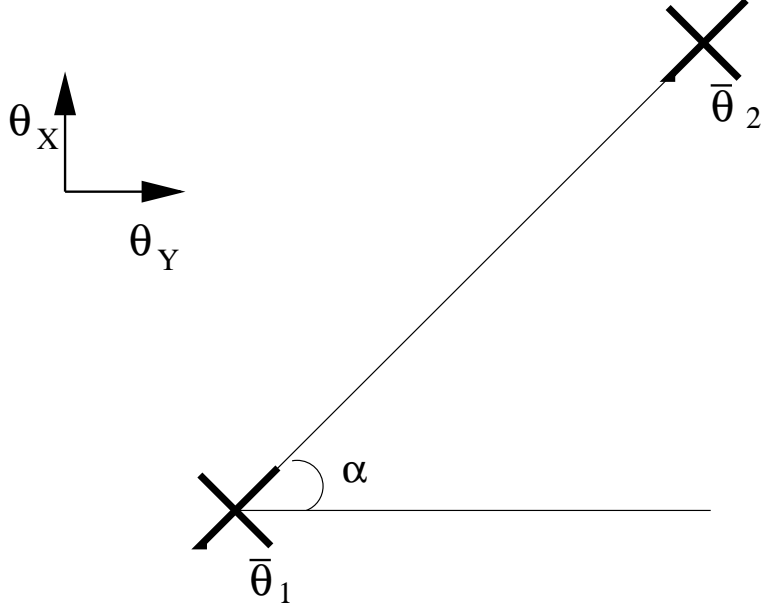


Fig. 5. Correlation functions for polarization are best defined for Stokes parameters Q_r and U_r measured with respect to axes aligned with the line connecting the two points being correlated.

Now suppose we have a given temperature/polarization map and then consider a parity inversion; e.g., consider a reflection about the x -axis. Then

$$\theta_y \rightarrow -\theta_y, \quad Q \rightarrow Q, \quad U \rightarrow -U, \quad l_x \rightarrow l_x, \quad l_y \rightarrow -l_y. \quad (24)$$

Also,

$$\tilde{T}(\vec{l}) \rightarrow \tilde{T}(\vec{l}), \quad \tilde{P}_G(\vec{l}) \rightarrow \tilde{P}_G(\vec{l}), \quad \tilde{P}_C(\vec{l}) \rightarrow -\tilde{P}_C(\vec{l}). \quad (25)$$

In other words, G and T are parity even, while C is parity odd. Thus, if the physics that gives rise to T/P fluctuations is parity conserving, we expect

$$C_l^{\text{TC}} = C_l^{\text{GC}} = 0, \quad \text{parity invariance} \quad (26)$$

in which case the statistics of the T/P map is determined entirely by the four power spectra, $C_l^{\text{TT}}, C_l^{\text{TG}}, C_l^{\text{GG}}$, and C_l^{CC} .

4. Correlation functions

For a temperature map, the correlation between the temperature $T(\vec{\theta}_1)$ and $T(\vec{\theta}_2)$ at any two points is

$$\langle T(\vec{\theta}_1)T(\vec{\theta}_2) \rangle = C_{\text{TT}}(|\vec{\theta}_1 - \vec{\theta}_2|), \quad (27)$$

and the correlation function $C_{\text{TT}}(\theta)$ depends only on the distance θ between the two points. The same is not true for Q and U . Since Q and U are not rotational invariants, their correlations will depend also on the orientation of the line connecting

the two points. Instead, one can define rotationally invariant correlation functions by considering the components Q_r and U_r of the polarization defined with respect to the line connecting the two points (Fig. 5). We can then define the correlation functions,

$$\langle Q_r(\vec{\theta}_1)Q_r(\vec{\theta}_2) \rangle = C_{\text{QQ}}(|\vec{\theta}_1 - \vec{\theta}_2|), \quad (28)$$

$$\langle U_r(\vec{\theta}_1)U_r(\vec{\theta}_2) \rangle = C_{\text{UU}}(|\vec{\theta}_1 - \vec{\theta}_2|), \quad (29)$$

$$\langle Q_r(\vec{\theta}_1)U_r(\vec{\theta}_2) \rangle = C_{\text{QU}}(|\vec{\theta}_1 - \vec{\theta}_2|). \quad (30)$$

Since $Q \rightarrow Q$ and $U \rightarrow -U$ under a parity inversion, $C_{\text{QU}} = 0$ if parity is conserved. If we correlate the polarization with temperature, then there are another three (TT,TQ,TU) correlation functions, one of which (TU) vanishes if parity is conserved.

The correlation functions can be written in terms of the power spectra,

$$C_{\text{QQ}}(\theta) + C_{\text{UU}}(\theta) = - \int_0^\infty \frac{l dl}{\pi} [C_l^{\text{GG}} + C_l^{\text{CC}}] J_0(l\theta), \quad (31)$$

$$C_{\text{QQ}}(\theta) - C_{\text{UU}}(\theta) = - \int_0^\infty \frac{l dl}{\pi} [C_l^{\text{GG}} - C_l^{\text{CC}}] J_4(l\theta), \quad (32)$$

where $J_\nu(x)$ are Bessel functions. These relations can also be inverted to give power spectra in terms of correlation functions. For derivations and details, see Refs. [10,11].

Finally, the correlation functions at zero lag give us the mean-square polarization,

$$\langle P^2 \rangle = \langle Q^2 + U^2 \rangle = \int_0^\infty \frac{l dl}{2\pi} [C_l^{\text{GG}} + C_l^{\text{CC}}] = \langle P_G^2 \rangle + \langle P_C^2 \rangle. \quad (33)$$

Exercise 3. Write an expression for the temperature power spectrum C_l^{TT} in terms of the temperature autocorrelation function $C^{\text{TT}}(\theta)$. Now do the same for the gradient and curl power spectra in terms of the QQ and UU autocorrelation functions.

5. Harmonic analysis on the full sky

If our maps extend beyond a small region of the sky, we will have to come to terms with the fact that the sky is a curved surface. Moreover, as we will see below, theoretical predictions for the power spectra will require solution of Boltzmann equations that require that we keep track of the distribution function for photons moving in all directions.

We thus generalize the tensor Fourier analysis (G and C) that we did above for STF 2×2 tensors that live on the 2-sphere. Our discussion in this Section follows Ref. [11]; a different but equivalent formalism is presented in Ref. [12]. In the usual spherical polar coordinates θ, ϕ , the sphere has a metric,

$$g_{ab} = \begin{pmatrix} 1 & 0 \\ 0 & \sin^2 \theta \end{pmatrix}. \quad (34)$$

The polarization tensor P_{ab} must be symmetric $P_{ab} = P_{ba}$ and trace-free $g^{ab}P_{ab} = 0$, from which it follows that,

$$P_{ab}(\hat{n}) = \frac{1}{2} \begin{pmatrix} Q(\hat{n}) & -U(\hat{n}) \sin \theta \\ -U(\hat{n}) \sin \theta & Q(\hat{n}) \sin^2 \theta \end{pmatrix}. \quad (35)$$

The factors of $\sin \theta$ also follow from the fact that the coordinate basis (θ, ϕ) is orthogonal but not orthonormal.

Let us now review some of the rules of differential geometry on the two-sphere. Covariant derivatives of scalar, vector, and tensor fields are

$$S_{;a} = S_{,a}, \quad V^a_{;b} = V^a_{,b} + V^c \Gamma_{bc}^a, \quad T^{ab}_{;c} = T^{ab}_{,c} + T^{db} \Gamma_{cd}^a + T^{ad} \Gamma_{cd}^b, \quad (36)$$

and ‘;’ denotes covariant derivative, $S_{,a} = (\partial S / \partial x^a)$, and the Christoffel symbols are

$$\Gamma_{bc}^a = \frac{1}{2} g^{ad} (g_{db,c} + g_{dc,b} - g_{bc,d}). \quad (37)$$

Also,

$$S^{;ab}{}_{ab} = \nabla^2 \nabla^2 S + R^{db} S_{;db} + \frac{1}{2} R^{;d} S_{;d}, \quad \nabla^2 S \equiv S^{;a}{}_{;a} \quad R_{ab} \equiv R^c{}_{acb}, \quad R \equiv R^a{}_{;a}. \quad (38)$$

Since the sphere has no boundary, we can integrate by parts,

$$\oint d^2 \hat{n} \sqrt{g} X^{ab} Y_{;ab} = - \oint d^2 \hat{n} \sqrt{g} X^{ab}{}_{;a} Y_{;b} = \oint d^2 \hat{n} \sqrt{g} X^{ab}{}_{;ab} Y, \quad (39)$$

where $Y(\hat{n})$ is a scalar function and $\oint d^2 \hat{n}$ denotes integration over the sphere. The antisymmetric tensor is

$$\epsilon_{ab} = \sqrt{g} \begin{pmatrix} 0 & 1 \\ -1 & 0 \end{pmatrix}, \quad (40)$$

and

$$\epsilon_{ca} \epsilon^c{}_b = g_{ab} = -\epsilon_{ac} \epsilon^c{}_b, \quad \epsilon_{ab} \epsilon_{cd} = g_{ac} g_{bd} - g_{ad} g_{bc}, \quad \epsilon_{ab;c} = 0. \quad (41)$$

Also, $\epsilon^{ab} T_{ab} = 0$ for a symmetric tensor, $T_{ab} = T_{ba}$.

For the two-sphere, the Riemann tensor is

$$R_{abcd} = \frac{1}{2} R \epsilon_{ab} \epsilon_{cd}, \quad R_{ab} = \frac{1}{2} R g_{ab}, \quad \epsilon^{ab} R_{abcd} = R \epsilon_{cd}, \quad \epsilon^{ac} R_{abcd} = \frac{1}{2} R \epsilon_{bd}. \quad (42)$$

For two STF tensors M_{ab}, N_{ab} (i.e. $g^{ab} M_{ab} = g^{ab} N_{ab} = \epsilon^{ab} M_{ab} = \epsilon^{ab} N_{ab} = 0$), the second of Eqs. (41) gives us

$$M^{ab} N^{cd} \epsilon_{ac} \epsilon_{bd} = -M^{ab} N_{ab}. \quad (43)$$

Also,

$$g = |g_{ab}| = \sin^2 \theta, \quad \epsilon_b^a = \begin{pmatrix} 0 & \sin \theta \\ -\csc \theta & 0 \end{pmatrix}, \quad (44)$$

$$\Gamma_{\phi\phi}^\theta = -\sin \theta \cos \theta, \quad \Gamma_{\theta\phi}^\phi = \Gamma_{\phi\theta}^\phi = \cot \theta, \quad (45)$$

and all other components vanish. Then, for a scalar function $Y(\hat{n})$,

$$\begin{aligned} Y_{;\theta\theta} &= Y_{,\theta\theta}, \\ Y_{;\theta\phi} &= Y_{,\theta\phi} - \cot\theta Y_{,\phi}, \\ Y_{;\phi\phi} &= Y_{,\phi\phi} + \sin\theta \cos\theta Y_{,\theta}. \end{aligned} \quad (46)$$

A symmetric rank-2 tensor M_{ab} has ‘divergence’,

$$\begin{aligned} M^{ab}{}_{;ab} &= M^{\theta\theta}{}_{,\theta\theta} + 2M^{\theta\phi}{}_{,\theta\phi} + M^{\phi\phi}{}_{,\phi\phi} - \sin\theta \cos\theta M^{\phi\phi}{}_{,\theta} \\ &+ 2\cot\theta M^{\theta\theta}{}_{,\theta} + 4\cot\theta M^{\theta\phi}{}_{,\phi} + (1 - 3\cos^2\theta)M^{\phi\phi} - M^{\theta\theta}, \end{aligned} \quad (47)$$

and ‘curl’,

$$\begin{aligned} M^{ab}{}_{;ac}\epsilon^c{}_b &= \sin\theta (M^{\theta\phi}{}_{,\theta\theta} + M^{\phi\phi}{}_{,\phi\theta}) - \csc\theta (M^{\theta\theta}{}_{,\theta\phi} + M^{\phi\theta}{}_{,\phi\phi}) - \cot\theta \csc\theta M^{\theta\theta}{}_{,\phi} \\ &+ 5\cos\theta M^{\theta\phi}{}_{,\theta} + 3\cos\theta M^{\phi\phi}{}_{,\phi} + 3(\cos\theta \cot\theta - \sin\theta) M^{\theta\phi}, \end{aligned} \quad (48)$$

Exercise 4. Verify Eqs. (47) and (48).

Any STF 2×2 tensor field can be written as the ‘gradient’ of some scalar field $A(\hat{n})$,

$$A_{;ab} - \frac{1}{2}g_{ab}A^c{}_c, \quad (49)$$

plus the ‘curl’ of some other scalar field $B(\hat{n})$,

$$\frac{1}{2}(B_{;ac}\epsilon^c{}_b + B_{;bc}\epsilon^c{}_a). \quad (50)$$

Just for comparison, a vector field is analogously decomposed as

$$V_a = \nabla_a A + \epsilon_{ab}\nabla_b B. \quad (51)$$

Since any scalar field on the sphere can be expanded in spherical harmonics (e.g. for the temperature),

$$\frac{T(\hat{n})}{T_0} = 1 + \sum_{l=1}^{\infty} \sum_{m=-l}^l a_{(lm)}^T Y_{(lm)}(\hat{n}), \quad (52)$$

where

$$a_{(lm)}^T = \frac{1}{T_0} \int d\hat{n} T(\hat{n}) Y_{(lm)}^*(\hat{n}), \quad (53)$$

it follows that the polarization tensor can be expanded in terms of basis functions that are gradients and curls of spherical harmonics,

$$\frac{\mathcal{P}_{ab}(\hat{n})}{T_0} = \sum_{l=2}^{\infty} \sum_{m=-l}^l \left[a_{(lm)}^G Y_{(lm)ab}^G(\hat{n}) + a_{(lm)}^C Y_{(lm)ab}^C(\hat{n}) \right]. \quad (54)$$

The expansion coefficients are given by

$$a_{(lm)}^{\text{G}} = \frac{1}{T_0} \int d\hat{n} \mathcal{P}_{ab}(\hat{n}) Y_{(lm)}^{\text{G}ab*}(\hat{n}), \quad a_{(lm)}^{\text{C}} = \frac{1}{T_0} \int d\hat{n} \mathcal{P}_{ab}(\hat{n}) Y_{(lm)}^{\text{C}ab*}(\hat{n}), \quad (55)$$

and

$$Y_{(lm)ab}^{\text{G}} = N_l \left(Y_{(lm):ab} - \frac{1}{2} g_{ab} Y_{(lm):c}{}^c \right), \quad (56)$$

$$Y_{(lm)ab}^{\text{C}} = \frac{N_l}{2} \left(Y_{(lm):ac} \epsilon^c{}_b + Y_{(lm):bc} \epsilon^c{}_a \right), \quad (57)$$

constitute a complete orthonormal set of basis functions for the G and C components of the polarization. The quantity,

$$N_l \equiv \sqrt{\frac{2(l-2)!}{(l+2)!}}, \quad (58)$$

is a normalization factor chosen so that

$$\int d\hat{n} Y_{(lm)ab}^{\text{G}*}(\hat{n}) Y_{(l'm')}^{\text{G}ab}(\hat{n}) = \int d\hat{n} Y_{(lm)ab}^{\text{C}*}(\hat{n}) Y_{(l'm')}^{\text{C}ab}(\hat{n}) = \delta_{ll'} \delta_{mm'}, \quad (59)$$

$$\int d\hat{n} Y_{(lm)ab}^{\text{G}*}(\hat{n}) Y_{(l'm')}^{\text{C}ab}(\hat{n}) = 0. \quad (60)$$

Also, we can integrate by parts to write alternatively,

$$a_{(lm)}^{\text{G}} = \frac{N_l}{T_0} \int d\hat{n} Y_{(lm)}^*(\hat{n}) \mathcal{P}_{ab}{}^{:ab}(\hat{n}), \quad (61)$$

$$a_{(lm)}^{\text{C}} = \frac{N_l}{T_0} \int d\hat{n} Y_{(lm)}^*(\hat{n}) \mathcal{P}_{ab}{}^{:ac}(\hat{n}) \epsilon_c{}^b. \quad (62)$$

Finally, since $\{\text{T}, \text{Q}, \text{U}\} \in \mathfrak{R}$,

$$a_{(lm)}^{\text{X}*} = (-1)^m a_{(l,-m)}^{\text{X}}, \quad (63)$$

where $\text{X} = \{\text{T}, \text{G}, \text{C}\}$.

Exercise 5. Consider a vector field V^a that lives on the surface of a two-dimensional sphere. Show that this vector field can be written as

$$V_a = \sum_{l=1}^{\infty} \sum_{m=-l}^l \left[a_{(lm)}^{\text{G}} Y_{(lm)a}^{\text{G}} + a_{(lm)}^{\text{C}} Y_{(lm)a}^{\text{C}} \right],$$

where $Y_{(lm)a}^{\text{G}}$ and $Y_{(lm)a}^{\text{C}}$ are gradient and curl vector spherical harmonics. Derive expressions for these harmonics and show that they are orthonormal.

The temperature/polarization power spectra are now

$$\left\langle a_{(lm)}^{\text{X}*} a_{(l'm')}^{\text{X}'} \right\rangle = C_l^{\text{XX}'} \delta_{ll'} \delta_{mm'}, \quad (64)$$

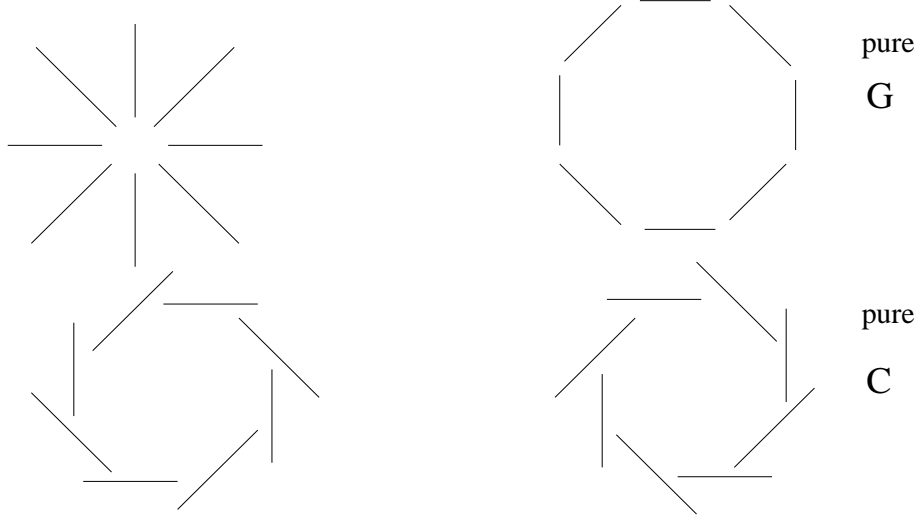


Fig. 6. Examples of G (top) and C (bottom) polarization patterns.

for $X, X' = \{T, G, C\}$. Of these six, two (TC and GC) are zero if parity is conserved.[§]

For future reference, the $Y_{(lm)ab}^G$ and $Y_{(lm)ab}^C$ are explicitly,

$$Y_{(lm)ab}^G(\hat{n}) = \frac{N_l}{2} \begin{pmatrix} W_{(lm)}(\hat{n}) & X_{(lm)}(\hat{n}) \sin \theta \\ X_{(lm)}(\hat{n}) \sin \theta & -W_{(lm)}(\hat{n}) \sin^2 \theta \end{pmatrix}, \quad (65)$$

and

$$Y_{(lm)ab}^C(\hat{n}) = \frac{N_l}{2} \begin{pmatrix} -X_{(lm)}(\hat{n}) & W_{(lm)}(\hat{n}) \sin \theta \\ W_{(lm)}(\hat{n}) \sin \theta & X_{(lm)}(\hat{n}) \sin^2 \theta \end{pmatrix}, \quad (66)$$

where

$$W_{(lm)}(\hat{n}) = \left(\frac{\partial^2}{\partial \theta^2} - \cot \theta \frac{\partial}{\partial \theta} + \frac{m^2}{\sin^2 \theta} \right) Y_{(lm)}(\hat{n}) = \left(2 \frac{\partial^2}{\partial \theta^2} + l(l+1) \right) Y_{(lm)}(\hat{n}), \quad (67)$$

and

$$X_{(lm)}(\hat{n}) = \frac{2im}{\sin \theta} \left(\frac{\partial}{\partial \theta} - \cot \theta \right) Y_{(lm)}(\hat{n}). \quad (68)$$

In terms of the spin-2 harmonics ${}_{\pm 2}Y_{(lm)}$ used in Refs. [12,13],

$$W_{(lm)}(\hat{n}) \pm iX_{(lm)}(\hat{n}) = \sqrt{\frac{(l+2)!}{(l-2)!}} {}_{\pm 2}Y_{(lm)}. \quad (69)$$

[§]Our GG, CC, and TG moments can be identified with the EE, BB, and TE moments of Ref. [12] through $a_{(lm)}^G = a_{lm}^E/\sqrt{2}$ and $a_{(lm)}^C = a_{lm}^B/\sqrt{2}$. Also, the C_l here reduce in the small-angle (large- l) limit with those in Section 4 as long as the angles in the flat-sky limit are given in radians; it is left as another exercise to the reader to verify this statement.

Note that if we replace (Q, U) by $(U, -Q)$, then $G \rightarrow C$ and $C \rightarrow -G$. This tells us therefore, that a pure-G polarization pattern becomes a pure-C pattern if we rotate each polarization vector by 45° , and *vice versa*. Examples of G and C type polarization patterns are shown in Fig. 6.

6. Correlation functions on the sphere

Correlation functions on the two-sphere are defined analogously to those on the flat sky. The line connecting the two points is now replaced by the great arc connecting the two points [11]. To calculate the two-point correlation functions, it is convenient to choose the north pole of the coordinate system to be one of the points. The temperature autocorrelation function is then

$$\begin{aligned}
C^{\text{TT}}(\theta) &= \left\langle \frac{T(0,0)}{T_0} \frac{T(\theta,0)}{T_0} \right\rangle \\
&= \sum_{lm'l'm'} \left\langle a_{(lm)}^{\text{T}*} a_{(l'm')}^{\text{T}} \right\rangle Y_{(lm)}^*(0,0) Y_{(l'm')}(\theta,0) \\
&= \sum_{lm'l'm'} C_l^{\text{TT}} \delta_{ll'} \delta_{mm'} \sqrt{\frac{2l+1}{4\pi}} \delta_{m0} Y_{(l'm')}(\theta,0) \\
&= \sum_l \frac{2l+1}{4\pi} C_l^{\text{TT}} P_l(\cos\theta). \tag{70}
\end{aligned}$$

For polarization, we need a bit more algebra. We begin by deriving expressions for the functions that appear in our definitions above of the tensor harmonics:

$$W_{(lm)}(\hat{n}) = -2 \sqrt{\frac{2l+1}{4\pi} \frac{(l-m)!}{(l+m)!}} G_{(lm)}^+(\cos\theta) e^{im\phi}, \tag{71}$$

$$iX_{(lm)}(\hat{n}) = -2 \sqrt{\frac{2l+1}{4\pi} \frac{(l-m)!}{(l+m)!}} G_{(lm)}^-(\cos\theta) e^{im\phi}, \tag{72}$$

with

$$G_{(lm)}^+(\cos\theta) \equiv - \left(\frac{l-m^2}{\sin^2\theta} + \frac{1}{2}l(l-1) \right) P_l^m(\cos\theta) + (l+m) \frac{\cos\theta}{\sin^2\theta} P_{l-1}^m(\cos\theta), \tag{73}$$

$$G_{(lm)}^-(\cos\theta) \equiv \frac{m}{\sin^2\theta} \left((l-1) \cos\theta P_l^m(\cos\theta) - (l+m) P_{l-1}^m(\cos\theta) \right). \tag{74}$$

The Legendre functions have the following asymptotic limits,

$$P_l^m(\cos\theta) \sim \frac{(-1)^{(m+|m|)/2}}{2^{|m|}|m|!} \frac{(l+|m|)!}{(l-|m|)!} \theta^{|m|}, \quad \theta \rightarrow 0 \quad (m \neq 0), \tag{75}$$

$$P_l^m(\cos\theta) \sim 1 - \frac{1}{4}l(l+1)\theta^2, \quad \theta \rightarrow 0. \tag{76}$$

We also note that at the north pole, $X_{lm}(\theta = 0) \neq 0$ and $W_{lm}(\theta = 0) \neq 0$ only for $m = 2$:

$$W_{(lm)}(0, 0) = \frac{1}{2} \sqrt{\frac{2l+1}{4\pi} \frac{(l+2)!}{(l-2)!}} (\delta_{m,2} + \delta_{m,-2}), \quad (77)$$

and

$$X_{(lm)}(0, 0) = \frac{i}{2} \sqrt{\frac{2l+1}{4\pi} \frac{(l+2)!}{(l-2)!}} (\delta_{m,2} - \delta_{m,-2}). \quad (78)$$

The QQ autocorrelation function is then defined as

$$C^{\text{QQ}}(\theta) = \left\langle \frac{Q_r(\hat{n}_1)}{T_0} \frac{Q_r(\hat{n}_2)}{T_0} \right\rangle_{\hat{n}_1 \cdot \hat{n}_2 = \cos \theta}, \quad (79)$$

where Q_r is measured with respect to the great arc connecting the two points. Let $Q(0, 0) \equiv \lim_{\theta \rightarrow 0} Q(\theta, 0)$. Then,

$$C^{\text{QQ}}(\theta) = \left\langle \frac{Q_r(0, 0)}{T_0} \frac{Q_r(\theta, 0)}{T_0} \right\rangle, \quad (80)$$

or

$$\begin{aligned} C^{\text{QQ}}(\theta) &= \left\langle \frac{Q(0, 0)}{T_0} \frac{Q(\theta, 0)}{T_0} \right\rangle \\ &= \sum_{lm'l'm'} N_l N_{l'} \left\langle \left[a_{(lm)}^{\text{G}} W_{(lm)}(0, 0) - a_{(lm)}^{\text{C}} X_{(lm)}(0, 0) \right] \right. \\ &\quad \left. \times \left[a_{(l'm')}^{\text{G}*} W_{(l'm')}^*(\theta, 0) - a_{(l'm')}^{\text{C}*} X_{(l'm')}^*(\theta, 0) \right] \right\rangle \\ &= \sum_l \sqrt{\frac{2l+1}{8\pi}} N_l [C_l^{\text{G}} (W_{(l2)}^* + W_{(l,-2)}^*) + i C_l^{\text{C}} (X_{(l2)}^* - X_{(l,-2)}^*)], \\ &= \sum_l \frac{2l+1}{2\pi} N_l^2 [C_l^{\text{G}} G_{l2}^+(\cos \theta) + C_l^{\text{C}} G_{l2}^-(\cos \theta)], \end{aligned} \quad (81)$$

where we have used in the first line,

$$Q(\hat{n}) = 2\mathcal{P}_{\theta\theta}(\hat{n}) = T_0 \sum_{l=2}^{\infty} \sum_{m=-l}^l N_l \left[a_{(lm)}^{\text{G}} W_{(lm)}(\hat{n}) - a_{(lm)}^{\text{C}} X_{(lm)}(\hat{n}) \right], \quad (82)$$

$$\begin{aligned} U(\hat{n}) &= -2 \csc \theta \mathcal{P}_{\theta\phi}(\hat{n}) \\ &= -T_0 \sum_{l=2}^{\infty} \sum_{m=-l}^l N_l \left[a_{(lm)}^{\text{G}} X_{(lm)}(\hat{n}) + a_{(lm)}^{\text{C}} W_{(lm)}(\hat{n}) \right]. \end{aligned} \quad (83)$$

Similarly, the UU correlation function is

$$C^{\text{UU}}(\theta) = \sum_l \frac{2l+1}{2\pi} N_l^2 [C_l^{\text{C}} G_{l2}^+(\cos \theta) + C_l^{\text{G}} G_{l2}^-(\cos \theta)], \quad (84)$$

and the TQ correlation function is

$$C^{\text{TQ}}(\theta) = \left\langle \frac{T(\hat{n}_1)}{T_0} \frac{Q_r(\hat{n}_2)}{T_0} \right\rangle_{\hat{n}_1 \cdot \hat{n}_2 = \cos \theta} = \sum_l \frac{2l+1}{4\pi} N_l C_l^{\text{TG}} P_l^2(\cos \theta). \quad (85)$$

Note again that the TU and QU correlation functions vanish if parity is conserved.

Exercise 6. If parity is broken, do the TU and QU correlation functions vanish? If not, calculate them in terms of the (parity-violating) power spectra.

7. Calculation of Predicted Power Spectra

Now that we have figured out how to describe the polarization field properly, let's proceed to see what theoretical models (e.g. primordial adiabatic density perturbations and gravitational waves) predict about the polarization. Since these calculations are extremely involved in practice, here we only outline the calculation. We will, however, be able to see precisely that gravitational waves produce a curl component, while density perturbations do not.

To begin, we follow the pioneering paper of Polnarev [14] to derive the angular distribution of photon intensities in the presence of a gravitational wave (GW). To begin, we suppose that the photons do not scatter. In this case, the photon energies are affected only by the form of the metric. Let us consider a single monochromatic plane-wave gravitational wave, which appears as a tensor perturbation to the FRW metric,

$$ds^2 = a^2(\eta)d\eta^2 - a^2(\eta)[dx^2(1+h_+) + dy^2(1-h_+) + dz^2], \quad (86)$$

where η is the conformal time and

$$h_+(\vec{x}, \eta) = h(\eta)e^{ik\eta}e^{-ikz}, \quad (87)$$

describes a plane wave propagating in the \hat{z} direction. This is a linearly-polarized gravitational wave with “+” (rather than “ \times ”) polarization. Here $h(\eta)$ is the amplitude; at early times when $k\eta \lesssim 1$, $h(\eta) \simeq \text{const}$, but then $h(\eta)$ redshifts away when $k\eta \gtrsim 1$ (see, e.g., Ref. [15]).

Exercise 7. Show that the amplitude $h_+(\eta)$ solves

$$\ddot{h}_+ + 2\frac{\dot{a}}{a}\dot{h}_+ + k^2h_+ = 0,$$

where the dot denotes derivative with respect to conformal time (actually, anisotropic stresses give something on the right-hand side, but we will neglect them). Then solve this equation for the case of pure matter domination and for pure radiation domination. (Your solution should be consistent with a gravitational-wave energy density $\rho_{\text{GW}} \propto a^{-4}$ with the scale factor $a(t)$ of the Universe when the mode wavelengths are smaller than the horizon.) Think about what the spectrum of gravitational waves should be in the Universe today, assuming an initially scale-free spectrum. You should find that the slope of the spectrum changes at the scale that entered

the horizon at matter-radiation equality. The spectrum is plotted in Fig. 3 of Ref. [16], and you should be able to understand the result plotted there analytically.

With this metric $[g_{\alpha\beta} = a^2 \text{diag}(1, -(1+h_+), -(1-h_+), -1)]$, the zeroth component P^0 of the photon four-momentum is the photon energy E multiplied by the scale factor $P^0 = aE$; P^0 is constant if $h_+ = 0$. We take $h \ll 1$ for small-amplitude gravitational waves.

Using the geodesic equation,

$$\frac{d^2 x^\mu}{d\lambda^2} = -\Gamma_{\alpha\beta}^\mu \frac{dx^\alpha}{d\lambda} \frac{dx^\beta}{d\lambda}, \quad (88)$$

$$P^\alpha = \frac{dx^\alpha}{d\lambda}, \quad \frac{d}{d\lambda} = \frac{dx^0}{d\lambda} \frac{d}{dx^0} = \frac{d\eta}{d\lambda} \frac{d}{d\eta} = P^0 \frac{d}{d\eta}, \quad (89)$$

and $g_{\mu\nu} P^\mu P^\nu = 0$ for photons, we arrive at the Sachs-Wolfe effect for this spacetime (to first order in h),

$$\frac{1}{P^0} \frac{dP^0}{d\eta} = \frac{1}{2} a^2 \frac{\partial h_+}{\partial \eta} (e_x^2 - e_y^2), \quad (90)$$

where $e_x = (1 - \mu^2)^{1/2} \cos \phi$ and $e_y = (1 - \mu^2)^{1/2} \sin \phi$ are the components of the direction of the photon momentum, and $\mu = \cos \theta$ and ϕ describe the photon direction.

Exercise 8. Verify Eq. (90).

Replacing P^0 by the comoving photon frequency $\nu = P^0 = a\nu_{phys} = \text{const}$, we find that the gravitational wave induces angular intensity variations of the form,

$$\frac{d\nu}{\nu d\eta} = -\frac{1}{2} (1 - \mu^2) \cos 2\phi e^{-ikz} \frac{d}{d\eta} (h e^{ik\eta}). \quad (91)$$

Now let us consider Thomson scattering of these photons by electrons. Scattering will change this angular distribution and it may induce polarization as well. To include the effect of Thomson scattering, we (following Polnarev 1986 [14]) consider an alternative set of ‘‘Stokes parameters’’, and describe the state of the radiation propagating in any given direction \hat{n} by the ‘‘vector’’,

$$\tilde{I} = \begin{pmatrix} I_\theta \\ I_\phi \\ U \end{pmatrix}, \quad (92)$$

where $I_\theta = a_\theta^2$, $I_\phi = a_\phi^2$, $Q = I_\theta - I_\phi$, and $I = I_\theta + I_\phi$, and Q and U are measured with respect to the $\hat{\theta}$ - $\hat{\phi}$ axes on the plane tangent to the sky at any given direction $\hat{n} = (\theta, \phi)$.

The distribution function \tilde{f} for photons is now also a ‘‘vector’’. For example, in a homogeneous universe, it is

$$\tilde{f} = f_0(\nu) \begin{pmatrix} 1 \\ 1 \\ 0 \end{pmatrix} = \tilde{f}_0(\theta, \phi), \quad (93)$$

where

$$f_0(\nu) = \frac{1}{e^{h\nu/kT} - 1} \quad (94)$$

is the usual blackbody distribution function, and the form (1 1 0) indicates no polarization. In the presence of the gravitational wave, there will be a perturbation, as determined above, so

$$\tilde{f}(\theta, \phi) = f_0 \left[\begin{pmatrix} 1 \\ 1 \\ 0 \end{pmatrix} + \tilde{f}_1 \right]. \quad (95)$$

Note that \tilde{f}_1 is a three-component “vector”, and it is most generally a function of conformal time η , position \vec{x} , frequency ν , and photon direction $(\theta, \phi) = \hat{n}$.

As the Universe expands, photons get re-distributed in frequency, polarization, and direction by the redshift due to the gravitational wave and also by Thomson scattering. Until now we have considered only the gravitational redshift and neglected scattering, which we now proceed to include. The time evolution of the photon distribution function is determined by the equation of radiative transfer, essentially the Boltzmann equation for the photon distribution function,

$$\frac{d\tilde{f}}{d\eta} = \frac{\partial\tilde{f}}{\partial\eta} + \hat{n}^i \frac{\partial\tilde{f}}{\partial x^i} = -\frac{\partial\tilde{f}}{\partial\nu} \frac{\partial\nu}{\partial\eta} - g(\tilde{\eta} - \tilde{J}), \quad (96)$$

where $g = \sigma_T n_e a$ is the scattering rate, n_e the electron density, and

$$\tilde{J} = \frac{1}{4\pi} \int_{-1}^1 d\mu' \int_0^{2\pi} d\phi' \tilde{P}(\mu, \phi, \mu', \phi') \tilde{f}(\eta, x^i, \nu, \mu', \phi'), \quad (97)$$

where

$$\tilde{P} = \begin{pmatrix} \mu^2 \mu'^2 \cos 2(\phi' - \phi) & -\mu^2 \cos 2(\phi' - \phi) & \mu^2 \mu' \sin 2(\phi' - \phi) \\ -\mu^2 \cos 2(\phi' - \phi) & \cos 2(\phi' - \phi) & -\mu \sin 2(\phi' - \phi) \\ -2\mu \mu'^2 \sin 2(\phi' - \phi) & 2\mu \sin 2(\phi' - \phi) & 2\mu \mu' \cos 2(\phi' - \phi) \end{pmatrix} \quad (98)$$

is the scattering matrix. Eq. (96) says that the total time derivative of the photon distribution function (written as an explicit time derivative plus the time evolution due to photon motion) is given by gravitational redshift (the first term on the right-hand side) in the perturbed spacetime plus the change due to Thomson scattering (the second term on the right-hand side) of photons from electrons. The quantity \tilde{J} is the angular intensity-polarization distribution that arises after the radiation has been Thomson scattered once from an initial distribution \tilde{f} . The scattering matrix \tilde{P} looks messy, but it simply tells us how an initial intensity-polarization pattern is re-arranged after Thomson scattering once from unpolarized electrons. It is straightforward to derive it from the angular-polarization dependence of Thomson scattering,

$$\frac{d\sigma_T}{d\Omega} \propto |\hat{\epsilon} \cdot \hat{\epsilon}'|^2; \quad (99)$$

see Refs. [14] and [9] for details.

The gravitational wave imprints at first an angular intensity pattern,

$$\frac{1}{\nu} \frac{d\nu}{d\eta} = -\frac{1}{2}(1 - \mu^2) \cos 2\phi e^{-ikz} \frac{d}{d\eta} (h e^{ik\eta}). \quad (100)$$

This intensity pattern is then altered when the photons undergo Thomson scattering. Before Thomson scattering, the intensity-polarization distribution function is the unperturbed distribution \tilde{f}_0 plus a small perturbation proportional to

$$\tilde{a} \equiv \frac{1}{2} \begin{pmatrix} 1 \\ 1 \\ 0 \end{pmatrix} (1 - \mu^2) \cos 2\phi, \quad (101)$$

due to the gravitational wave. After Thomson scattering, the angular intensity-polarization distribution is altered; the scattering matrix above then introduces a second component to the perturbation proportional to

$$\tilde{b} \equiv \begin{pmatrix} (1 + \mu^2) \cos 2\phi \\ -(1 + \mu^2) \cos 2\phi \\ 4\mu \sin 2\phi \end{pmatrix}, \quad (102)$$

One might guess that subsequent scatterings would add further more complicated angular dependence to the distribution function. However, as first noted by Polnarev [14], Thomson scattering of a distribution function of the form \tilde{b} returns a distribution function of the form \tilde{a} . In other words, the basis functions \tilde{a} and \tilde{b} form a closed basis under Thomson scattering. This is simply a consequence of the time-reversal invariance of the scattering process: If Thomson scattering converts a distribution \tilde{a} to a distribution \tilde{b} , then it should turn a distribution \tilde{b} into a distribution \tilde{a} .

The linearized solution to the Boltzmann equation, including fully the effects of gravitational redshift and Thomson scattering, in the presence of a gravitational wave must therefore be of the form

$$\tilde{f} = \tilde{f}_0 + e^{-ikz + ik\eta} \tilde{f}_1, \quad (103)$$

where the perturbation is

$$\tilde{f}_1 = \alpha(\eta, \nu_0, \mu) \tilde{a} + \beta(\eta, \nu_0, \mu) \tilde{b}. \quad (104)$$

Here, $\alpha(\eta, \nu_0, \mu)$ and $\beta(\eta, \nu_0, \mu)$ are coefficients that must be determined by solution of the Boltzmann equation.

Defining an ‘‘anisotropy’’ $A = \xi(1 - \mu^2)$ with $\xi \equiv \alpha + \beta$, and ‘‘polarization’’ $\Pi = \beta(1 + \mu^2)$ (which is nonzero only if there is polarization), the radiative-transfer equation can be re-written,

$$\begin{aligned} \dot{\xi} + [ik(1 - \mu) + g]\xi &= \frac{1}{f_0} \frac{df_0(\nu_0)}{d\nu_0} \left(\frac{dh}{d\nu} + ikh \right), \\ \dot{\beta} + [ik(1 - \mu) + g]\beta &= \frac{3}{16} g \int d\mu' [(1 + \mu'^2)^2 \beta - \frac{1}{2} \dot{\xi} (1 - \mu'^2)^2]. \end{aligned} \quad (105)$$

The first equation generates a temperature fluctuation from the gravitational wave, and the second generates polarization through scattering of that temperature fluctuation.[¶]

Eqs. (105) are a set of coupled partial differential equations for the time (η) and angular (μ) dependence of the distribution functions $\xi(\eta, \mu)$ and $\beta(\eta, \mu)$. In practice, these are solved numerically by Legendre transforming $\xi(\eta, \mu) \rightarrow \xi_l(\eta)$ and $\beta(\eta, \mu) \rightarrow \beta_l(\eta)$ through

$$\xi_l(\eta) = \frac{1}{2} \int_{-1}^1 d\mu \xi(\eta, \mu) P_l(\mu), \quad (106)$$

$$\beta_l(\eta) = \frac{1}{2} \int_{-1}^1 d\mu \beta(\eta, \mu) P_l(\mu). \quad (107)$$

The partial differential equations for $\xi(\eta, \mu)$ and $\beta(\eta, \mu)$ then become an infinite set^{||} of coupled differential equations for $\xi_l(\eta)$ and $\beta_l(\eta)$ which are propagated numerically from some very early time (where the solutions are analytically determined in the so-called tight-coupling approximation) to the present time.

Exercise 9. Derive the differential equations for $\xi_l(\eta)$ and $\beta_l(\eta)$; this is not necessarily an easy problem. If you want to go further, you can determine the early-time solutions to these equations using the tight-coupling approximation, in which the scattering rate $g = n_e \sigma_T a$ is assumed to be huge.

We will not discuss the numerical techniques (which are highly nontrivial) here, but will show results a bit later. For our purposes, we simply need to know that the angular polarization pattern induced by this gravitational wave can now be written,

$$\begin{aligned} Q(\theta, \phi) &= \frac{1}{4} T_0 \sum_l (2l+1) P_l(\cos \theta) (1 + \cos^2 \theta) \cos 2\phi \xi_l, \\ U(\theta, \phi) &= \frac{1}{4} T_0 \sum_l (2l+1) P_l(\cos \theta) 2 \cos \theta \sin 2\phi \xi_l. \end{aligned} \quad (108)$$

We then get a polarization tensor,

$$\begin{aligned} P^{ab}(\theta, \phi) &= \frac{T_0}{8} \sum_l (2l+1) P_l(\cos \theta) \xi_l \\ &\times \begin{pmatrix} (1 + \cos^2 \theta) \cos 2\phi & -2 \cot \theta \sin 2\phi \\ -2 \cot \theta \sin 2\phi & -(1 + \cos^2 \theta) \csc^2 \theta \cos 2\phi \end{pmatrix}. \end{aligned} \quad (109)$$

Exercise 10. Verify Eq. (108). This should be easy.

[¶]Note that the factor $ik(1 - \mu)$ that appears in Eqs. (105) often appears elsewhere simply as $ik\mu$. The reason traces back to the fact that Polnarev writes $h_{\pm} \propto h(\eta)e^{ik\eta}$ and $\tilde{f} = \tilde{f}_0 + \tilde{f}_1 e^{-ikz+ik\eta}$ while other authors usually write $h_{\pm} \propto h(\eta)$ and $\tilde{f} = \tilde{f}_0 + \tilde{f}_1$. We thank J. Pritchard for clarifying this point.

^{||}These are truncated at some large value of l ; the truncation procedure is not trivial; see, e.g., Ref. [17].

If we now expand Eq. (109) in tensor spherical harmonics, the resulting tensor-harmonic coefficients are

$$a_{lm}^G = \frac{1}{8} N_l \sum_j (2j+1) \xi_j \int d\hat{n} Y_{lm}^*(\hat{n}) M_{(j):ab}^{ab}(\hat{n}), \quad (110)$$

which after a little bit of algebra becomes

$$a_{lm}^G = \frac{1}{8} (\delta_{m,2} + \delta_{m,-2}) \sqrt{2\pi(2l+1)} \times \left[\frac{(l+2)(l+1)\xi_{l-2}}{(2l-1)(2l+1)} + \frac{6l(l+1)\xi_l}{(2l+3)(2l-1)} + \frac{l(l-1)\xi_{l+2}}{(2l+3)(2l+1)} \right]. \quad (111)$$

Likewise,

$$a_{lm}^C = \frac{1}{8} N_l \sum_j (2j+1) \xi_j \int d\hat{n} Y_{lm}^*(\hat{n}) M_{(j):ac}^{ab}(\hat{n}) \epsilon_b^c \quad (112)$$

$$= \frac{-i}{4} \sqrt{\frac{2\pi}{(2l+1)}} (\delta_{m,2} - \delta_{m,-2}) [(l+2)\xi_{l-1} + (l-1)\xi_{l+1}]. \quad (113)$$

We have thus shown explicitly that both the G and C components are nonzero for a gravitational wave.

We get the contributions to the power spectra C_l^{GG} and C_l^{CC} from this particular gravitational wave (in the \hat{z} direction with ‘+’ polarization) from

$$C_l^{\text{GG}} = \frac{1}{2l+1} \sum_m |a_{lm}^G|^2 = \frac{\pi}{16} \left[\frac{(l+2)(l+1)\xi_{l-2}}{(2l-1)(2l+1)} + \frac{6l(l+1)\xi_l}{(2l+3)(2l-1)} + \frac{l(l-1)\xi_{l+2}}{(2l+3)(2l+1)} \right]^2 \quad (114)$$

and similarly for C_l^{CC} . Summing over all Fourier modes, $\int d^3k/(2\pi)^3$, and over both polarization states, the final result for C_l^{GG} is

$$C_l^{\text{GG}} = \frac{1}{16\pi} \int k^2 dk \left[\frac{(l+2)(l+1)\xi_{l-2}}{(2l-1)(2l+1)} + \frac{6l(l+1)\xi_l}{(2l+3)(2l-1)} + \frac{l(l-1)\xi_{l+2}}{(2l+3)(2l+1)} \right]^2, \quad (115)$$

and similarly for C_l^{CC} . Note, finally, that the cross-correlation power spectrum vanishes

$$C_l^{\text{GC}} = \sum_{m=-l}^{m=l} \frac{a_{lm}^{G*} a_{lm}^C}{2l+1} = 0, \quad (116)$$

as it should. This is because $a_{lm}^G \propto (\delta_{m,2} + \delta_{m,-2})$, while $a_{lm}^C \propto (\delta_{m,2} - \delta_{m,-2})$.

Now what about scalar (density) perturbations? By following steps similar to those above, one can show that they do not produce a curl component in the CMB polarization. Here we only sketch the calculation and leave out details. Again, consider a single Fourier mode of the density field in the \hat{z} direction. Then the

Sachs-Wolfe effect induces an intensity variation proportional to $(\cos^2 \theta - 1/3)$, so now

$$\tilde{f}_1 = \alpha(\eta, \nu_0, \mu)\tilde{a} + \beta(\eta, \nu_0, \mu)\tilde{b}, \quad (117)$$

with

$$\tilde{a} = \left(\mu^2 - \frac{1}{3}\right) \begin{pmatrix} 1 \\ 1 \\ 0 \end{pmatrix}, \quad \tilde{b} = (1 - \mu^2) \begin{pmatrix} 1 \\ -1 \\ 0 \end{pmatrix}. \quad (118)$$

We thus find that for $\vec{k} \parallel \hat{z}$, $U(\hat{n}) = 0$, so

$$M_{(j)}^{ab}(\theta, \phi) = \sin^2 \theta P_j(\cos \theta) \begin{pmatrix} 1 & 0 \\ 0 & \frac{-1}{\sin^2 \theta} \end{pmatrix}. \quad (119)$$

One finds $a_{lm}^G \neq 0$, but $a_{lm}^C = 0$. This follows because $M_{:ac}^{ab}\epsilon_b^c = 0$ which follows since $M_{:ac}^{ab}$ is diagonal and independent of ϕ . Therefore, if one detects a curl component in the CMB, it is a signature for primordial gravitational waves (see Fig. 7).

Exercise 11. Show that if the gravitational-wave background is composed entirely of gravitational waves with right-handed circular polarization (and no left-handed gravitational waves) that $C_l^{\text{TC}} \neq 0$; i.e., that there is a cross-correlation between the CMB temperature and the gradient component of the polarization. (Hint: Consider a single circularly-polarized gravitational wave propagating in the \hat{z} direction; from Ref. [18].)

8. Comments on power spectra

The power spectra shown in Fig. 7 show a variety of features. The origin of these features, as well as their dependence on cosmological parameters, has been the subject of much study. We will not discuss them in detail but refer the reader to the reviews and books listed in the Introduction for more details. Here, we point out only a few interesting and relevant features.

- There are acoustic peaks in the GG power spectrum for density perturbations. These are out of phase from the peaks in the TT power spectrum. The temperature fluctuation is due primarily to density fluctuations at the surface of last scattering, and secondarily to the peculiar velocity at the surface of last scattering. The peaks in C_l^{TT} are due to the density perturbations; the troughs are filled in by peculiar velocities, which oscillate (just as in an ordinary harmonic oscillator) out of phase by 90° .

Before recombination, the electrons and photons are tightly coupled, so the electrons see no quadrupole in the photon intensity and thus produce no polarization. Just before recombination, the photons begin to have longer path lengths as they begin to decouple. Since this nonequilibrium process depends on the time derivative of the baryon density (just like the velocity does), the polarization is out of phase with the density, and in phase with the velocity [19].

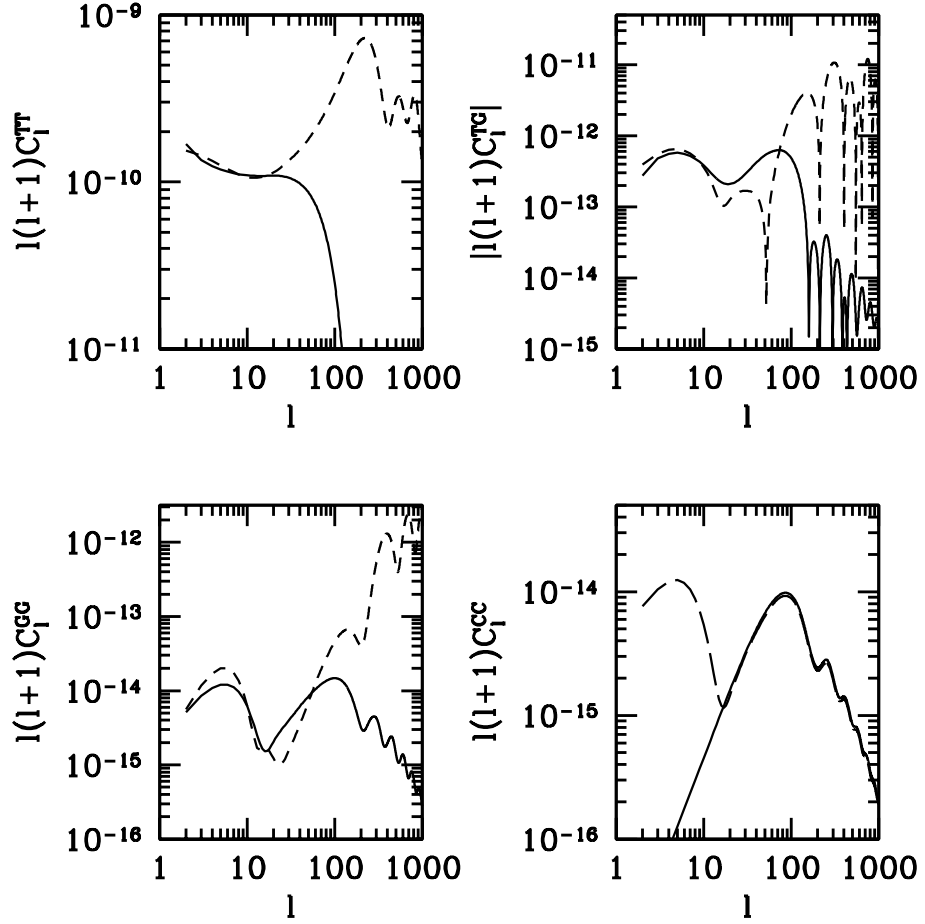


Fig. 7. Power spectra of temperature and polarization (G and C) and cross-spectrum TG for scalar perturbations (dotted line) and perturbations due to gravitational waves (solid line). Note that the power spectrum of ‘curl’ component C, due to scalar perturbations, is missing, and the dashed line corresponds a reionized model with optical depth $\tau = 0.166$ to the surface of last scattering.

- The power spectra due to gravitational waves drop precipitously for $l \gtrsim 100$. This is because on smaller scales, the gravitational waves have entered the horizon and had time for their amplitudes to redshift away by the time of recombination.
- Reionization induces a large bump in C_l^{GG} , C_l^{CC} , and C_l^{TG} at $l \lesssim 10$ [20]. This is simply due to scattering of the quadrupole by reionized gas. A rough estimate for the l of this peak can be obtained by assuming an Einstein–de Sitter Universe and noting then that

$$l_{\text{reion}} \sim 200 \left(\frac{z_{\text{reion}}}{z_{\text{rec}}} \right)^{1/2} \frac{1}{\sqrt{3}} \sim 10 \quad \text{for } z_{\text{reion}} \sim 10, \quad (120)$$

where $l \sim 200$ is the acoustic-peak location, and we have used the approximation that the sound speed $c_s \simeq c/\sqrt{3}$ in the primordial plasma is dominated by radiation.

- C_l^{GG} from density perturbations peaks at $l \sim 1000$, as opposed to $l \sim 200$ for C_l^{TT} : there is more power on small scales in the polarization. This is because polarization induced by a particular Fourier mode of the primordial density field depends on the gradient of that density field.
- The amplitude of C_l^{CC} is proportional to the square of the amplitude of the gravitational-wave background, which is fixed by the height of the inflaton potential during inflation. This can be quantified by

$$J \equiv 6C_2^{\text{TT,tensor}} \simeq 10^{-10} \frac{V}{(3 \times 10^{16} \text{ GeV})^4}, \quad (121)$$

where V is the inflaton-potential height during inflation, and $C_2^{\text{TT,tensor}}$ is the tensor (gravitational-wave) contribution to the temperature quadrupole. Since the latter is $\sim 10^{-10}$, we already know that the energy scale of inflation is $V^{1/4} \lesssim 3 \times 10^{16} \text{ GeV}$. The curl component of the CMB polarization induced by gravitational waves is thus proportional to the scale-height of inflation:

$$C_l^{\text{CC}} \propto V. \quad (122)$$

Therefore, detection of a curl component in the CMB due to gravitational waves would provide not only a “smoking gun” for inflation, but it would also tell us the height of the inflaton potential during inflation, and thus provide some hints as to the new physics responsible for inflation. In practice, any realistic CMB polarization experiment will be able to detect the GW-induced CMB curl component only if $V \gtrsim 10^{15} \text{ GeV}$; in other words, only if inflation took place at the energy scale of grand unification.

- C_l^{CC} from gravitational waves peaks at $l \sim 100$ or at $\sim 2^\circ$. If there is no other sources of a curl component (see below), then detection of the curl component is not cosmic-variance limited.

- Gravitational waves contribute a roughly scale-invariant temperature power spectrum C_l^{TT} at low l , just like density perturbations. However, cosmic variance removes our ability to detect an excess of $\lesssim 10\%$ over the density-perturbation contribution to C_l^{TT} , even if we could predict theoretically the density-perturbation amplitude.
- If there is no other source of a curl component, and if the large-angle polarization bump due to reionization is not big, then the optimal survey strategy [21] entails a deep integration on a $\sim 5^\circ \times 5^\circ$ patch of sky, with an angular resolution $\lesssim 1^\circ$ fwhm. This is the strategy of experiments like BICEP and QUIET. We now know from the WMAP detection of a large-angle temperature-polarization correlation that the reionization bump is probably quite big. In this case, an all-sky experiment with roughly the same instrumental sensitivity (noise-equivalent temperature) might have similar sensitivity to inflationary gravitational waves.

Exercise 11. Scale-invariant spectra of density perturbations and of gravitational waves each produce a nearly scale-invariant spectrum, $l(l+1)C_l^{\text{TT,tensor}} \simeq \text{constant}$, in the CMB at large scales (i.e., $l \gtrsim 20$). Suppose that most of the observed anisotropy at large scales comes from density perturbations, and pretend that we knew precisely the amplitude of the density-perturbation power spectrum from modeling smaller-scale fluctuations, other observations, or divine inspiration. If so, there would be a limit, set by cosmic variance, to the smallest gravitational-wave amplitude (quantified by, e.g., $6C_2^{\text{TT,tensor}}$, the gravitational-wave contribution to the temperature quadrupole moment) that could be determined from the measured CMB power spectrum. Estimate the smallest detectable value of $C_2^{\text{TT,tensor}}$. You will need to start by showing that the 1σ cosmic-variance error with which each C_l^{TT} can be measured is $\sqrt{2/(2l+1)}C_l^{\text{TT}}$.

9. Gravitational Lensing (Cosmic Shear) and CMB Polarization

Above we showed that density perturbations do not induce a curl in the polarization, and thus concluded that detection of a curl in the CMB polarization automatically implies detection of gravitational waves. However, that derivation assumed only linear perturbations, in which each Fourier mode of the density field is considered independently. If more than one Fourier mode of the density field is considered, then different modes can interact and produce a curl, even without gravitational waves. Since $\delta \sim 10^{-5}$ at the last-scattering surface, this density-perturbation-induced curl component should be small.

We do know, however, that the observed CMB temperature-polarization map will be distorted by *cosmic shear* (CS), gravitational lensing by large-scale mass inhomogeneities between us and the surface of last scattering. The effect of cosmic shear is to displace the temperature and polarization from a given direction $\vec{\theta}$ at

the surface of last scattering to an adjacent position, $\vec{\theta} + \delta\vec{\theta}$:

$$\begin{pmatrix} T \\ Q \\ U \end{pmatrix}_{obs.}(\vec{\theta}) = \begin{pmatrix} T \\ Q \\ U \end{pmatrix}_{ls}(\vec{\theta} + \delta\vec{\theta}) \simeq \begin{pmatrix} T \\ Q \\ U \end{pmatrix}_{ls}(\vec{\theta}) + \delta\vec{\theta} \cdot \nabla \begin{pmatrix} T \\ Q \\ U \end{pmatrix}_{ls}(\vec{\theta}), \quad (123)$$

where $\delta\vec{\theta} = \nabla\varphi$ is the cosmic-shear deflection angle, and

$$\varphi(\hat{n}) = -2 \int_0^{r_{ls}} dr \frac{d_A(r_0 - r)}{d_A(r)d_A(r_0)} \Phi(r, \hat{n}r) \quad (124)$$

is the projection of the gravitational potential $\Phi(r, \hat{n}r)$ (obtained from the mass distribution through the Poisson equation) along the line of sight, and $d_A(r)$ is the angular-diameter distance corresponding to the comoving radial coordinate r .

Noting that

$$\frac{l_x^2 - l_y^2}{l_x^2 + l_y^2} = \cos 2\phi_l, \quad \frac{2l_x l_y}{l_x^2 + l_y^2} = \sin 2\phi_l, \quad (125)$$

our previous transformation [cf., Eq. (18)] between (Q, U) and (G, C) is (using G and C as a shorthand for \tilde{P}_G and \tilde{P}_C , respectively),

$$\begin{pmatrix} G \\ C \end{pmatrix}(\vec{l}) = \frac{1}{2} \begin{pmatrix} \cos 2\phi_l & \sin 2\phi_l \\ \sin 2\phi_l & -\cos 2\phi_l \end{pmatrix} \begin{pmatrix} Q \\ U \end{pmatrix}(\vec{l}). \quad (126)$$

Let us suppose the polarization field at the surface of last scattering has no curl; then this relation can be inverted to give

$$Q(\vec{l}) = 2G(\vec{l}) \cos 2\phi_l, \quad U(\vec{l}) = -2G(\vec{l}) \sin 2\phi_l, \quad (127)$$

and

$$\nabla Q(\vec{\theta}) = -2i \int \frac{d^2\vec{l}}{(2\pi)^2} G(\vec{l}) \cos 2\phi_l \vec{l} e^{-i\vec{l}\cdot\vec{\theta}}, \quad (128)$$

and similarly for $\nabla U(\vec{\theta})$ with $\cos \rightarrow -\sin$. The deflection angle is likewise

$$\varphi(\vec{\theta}) = -i \int \frac{d^2\vec{l}}{(2\pi)^2} \varphi(\vec{l}) e^{-i\vec{l}\cdot\vec{\theta}} \vec{l}. \quad (129)$$

Thus, the perturbation to Q and U induced by gravitational waves is

$$\delta Q(\vec{\theta}) = \nabla Q \cdot \nabla\varphi = \int \frac{d^2\vec{l}}{(2\pi)^2} e^{i\vec{l}\cdot\vec{\theta}} (\nabla Q \cdot \nabla\varphi)_{\vec{l}}, \quad (130)$$

where

$$\delta Q(\vec{l}) \equiv (\nabla Q \cdot \nabla\varphi)_{\vec{l}} = 2 \int \frac{d^2\vec{l}_1}{(2\pi)^2} [\vec{l}_1 \cdot (\vec{l} - \vec{l}_1)] G(\vec{l}_1) \varphi(\vec{l} - \vec{l}_1) \cos 2\phi_{\vec{l}_1}, \quad (131)$$

$$\delta U(\vec{l}) \equiv (\nabla U \cdot \nabla\varphi)_{\vec{l}} = -2 \int \frac{d^2\vec{l}_1}{(2\pi)^2} [\vec{l}_1 \cdot (\vec{l} - \vec{l}_1)] G(\vec{l}_1) \varphi(\vec{l} - \vec{l}_1) \sin 2\phi_{\vec{l}_1}. \quad (132)$$

Although the original map had (by assumption) no curl, the lensed map does:

$$\begin{aligned}
 C(\vec{l}) &= \frac{1}{2}[\sin 2\phi_{\vec{l}}Q(\vec{l}) - \cos 2\phi_{\vec{l}}U(\vec{l})] \\
 &= \int \frac{d^2\vec{l}_1}{(2\pi)^2} [\vec{l}_1 \cdot (\vec{l} - \vec{l}_1)] G(\vec{l}_1) \varphi(\vec{l} - \vec{l}_1) \sin 2(\phi_{\vec{l}} - \phi_{\vec{l}_1}) \\
 &= \int \frac{d^2\vec{l}_1}{(2\pi)^2} [\vec{l}_1 \cdot (\vec{l} - \vec{l}_1)] G(\vec{l}_1) \varphi(\vec{l} - \vec{l}_1) \sin 2\phi_{\vec{l}_1}. \tag{133}
 \end{aligned}$$

Thus, our earlier claim that detection of a curl component constitutes detection of a gravitational-wave background is not entirely valid, as we have just shown explicitly that a curl component can be induced by cosmic shear [22].

Using the power spectrum $\langle |\varphi_{\vec{l}}|^2 \rangle = C_l^{\varphi\varphi}$ for the projected potential, the power spectrum for the curl induced by lensing is,

$$C_l^{\text{CC}} = \int \frac{d^2\vec{l}_1}{(2\pi)^2} [\vec{l}_1 \cdot (\vec{l} - \vec{l}_1)]^2 \sin^2 2\phi_{\vec{l}_1} C_{|\vec{l}-\vec{l}_1|}^{\varphi\varphi} C_{l_1}^{\text{GG}}. \tag{134}$$

In Fig. 8 we show numerical results for the CMB polarization curl induced by cosmic shear (lensing) [23,24]. If the gravitational-wave amplitude (solid line) is large enough, the CS curl will not interfere with detection of gravitational waves, and the gravitational-wave signal can be distinguished from the lensing signal by the shape of the power spectrum. However, if the gravitational-wave amplitude is small ($\lesssim 4 \times 10^{15}$ GeV), lensing (dashed line) produces a background, and the gravitational-wave curl cannot be detected [23,24,25].

Fortunately, something can be done to help separate the CS-induced curl from the GW-induced curl. Seljak and Zaldarriaga [26], Hu and Okamoto [27], and others have shown that measurement of higher-order correlations induced by lensing can be used to reconstruct $\delta\vec{\varphi}(\vec{\theta})$, the deflection angle, as a function of position on the sky. Refs. [23,24] have then evaluated how well these may be used to reduce the CS-induced curl. This subtraction is somewhat involved technically, and still under active investigation. We give a very brief description here to provide the basic flavor of the technique; readers are referred to the original papers for more details.

In the absence of lensing each Fourier mode of the T (or Q or U) field is statistically independent:

$$\langle T(\vec{l})T(\vec{l}') \rangle = 0 \quad \text{for } \vec{l} \neq \vec{l}'. \tag{135}$$

However, if there is lensing, an observed Fourier mode $T(\vec{l})$ has contributions from all pairs of temperature and projected-potential Fourier modes $T(\vec{l}_1)$ and $\varphi(\vec{l}_2)$ that have $\vec{l} = \vec{l}_1 + \vec{l}_2$. Thus, with lensing,

$$\langle T(\vec{l})T(\vec{l}') \rangle = f(\vec{l}, \vec{l}') \varphi(\vec{L}) \quad \vec{l} \neq \vec{l}', \tag{136}$$

in the presence of some fixed projected potential $\varphi(\vec{\theta})$ with Fourier components $\varphi(\vec{L})$. Here,

$$f(\vec{l}, \vec{l}') = C_l^{\text{TT}}(\vec{L} - \vec{l}) + C_{l'}^{\text{TT}}(\vec{L} - \vec{l}'). \tag{137}$$

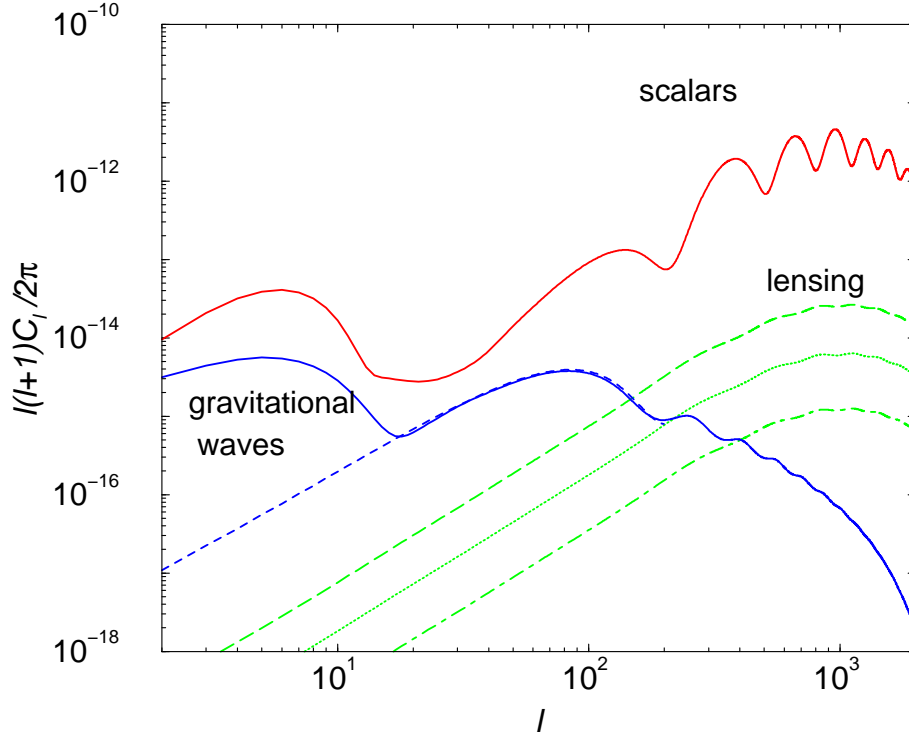


Fig. 8. Contributions to the CMB polarization power spectra. The upper (blue) solid “gravitational waves” curve is the curl component due to gravitational waves in the presence of reionization with an optical depth $\tau = 0.17$ (note the large-angle bump) and the associated (blue) dashed curve is that with no reionization. The amplitude of this curve is for the largest inflaton-potential height ($V \simeq 3.5 \times 10^{16}$ GeV) allowed by COBE; note that $C_l^{\text{CC,GW}} \propto V$, so the amplitude of this curve will be reduced accordingly if V is reduced. The short-dash (green) “lensing” curve is the curl power spectrum induced by cosmic shear (weak gravitational lensing due to density perturbations between us and the surface of last scattering). The red “scalar” curve is the GG power spectrum due to density perturbations (with reionization), shown here for reference. The dotted “lensing” (green) curve is the cosmic-shear contribution to the curl component that comes from structures out to a redshift $z = 1$, and the green “lensing” dot-dash curve is the residual cosmic-shear power spectrum left after subtraction with higher-order temperature-polarization correlations, as described in the text. From Ref. [23].

(There are analogous expressions for polarization, but for simplicity, we deal here only with T.) To determine a given \vec{L} component of φ , we simply sum over all pairs $T(\vec{l}_1)$, $T(\vec{l}_2)$ with $\vec{L} = \vec{l}_1 + \vec{l}_2$. In practice we have to weight these pairs taking into account noise from the random-field nature of the fluctuations, as well as instrument noise. Doing so, Hu-Okamoto find the following estimator for the Fourier components of the deflection angle,

$$\delta\vec{\theta}(\vec{L}) = \frac{i\vec{L}A(L)}{L^2} \int \frac{d^2\vec{l}_1}{(2\pi)^2} T(\vec{l}_1)T(\vec{l}_2)F(\vec{l}_1, \vec{l}_2), \quad (138)$$

$$F(\vec{l}_1, \vec{l}_2) \equiv \frac{f(\vec{l}_1, \vec{l}_2)}{2C_{l_1}^{\text{TT},t}C_{l_2}^{\text{TT},t}}, \quad A(L) = L^2 \left[\int \frac{d^2\vec{l}_1}{(2\pi)^2} f(\vec{l}_1, \vec{l}_2)F(\vec{l}_1, \vec{l}_2) \right]^{-1}, \quad (139)$$

and $C_l^{\text{TT},t}$ is the total observed (signal plus noise) power spectrum. Thus, with these estimators, the projected potential can be determined as a function of position across the sky from the measured temperature map. We can then use this projected-potential measurement to reconstruct the polarization pattern at the surface of last scattering from the (lensed) polarization pattern that is observed. Similar estimators that use the lensed polarization (rather than temperature) can also be constructed [27,28], but we do not include them as the expressions rapidly become unwieldy. The precision with which $\varphi(\vec{L})$ can be reconstructed depends on the number of small-scale coherence patches in the temperature-polarization map that can be used as ‘sources’ with which the shear can be reconstructed. Thus, high angular resolution and high sensitivity are required. Since the polarization power spectrum peaks at $l \sim 1000$, rather than $l \sim 200$, there are more small-scale coherence patches in the polarization than in the temperature. As a result, a high-sensitivity and high-resolution polarization map will be required for optimal lensing reconstruction. The degree to which the curl component induced by cosmic shear can be reduced depends on how well this reconstruction can be accomplished. For plausible assumptions about a post-Planck CMB polarization satellite (such as those that NASA is now considering), the CS-induced curl can be reduced by a factor ~ 10 in power-spectrum amplitude (as shown in Fig. 8). This requires a full-sky map of the temperature and polarization with an angular resolution $\theta_{\text{fwhm}} \sim \text{arcmins}$ and detector noise-equivalent temperature $s \sim 1\mu\text{K}\sqrt{\text{sec}}$. Higher-order correlations may improve upon this subtraction by a bit more [29,30].

Exercise 13. Show that the estimators given in Eqs. (138) and (139) are the minimum-variance estimators for the projected potential that can be constructed from the temperature map. You may need to go to the original papers to see how this is done.

The best strategy to detect inflationary gravitational waves is now a subject of some study. If a curl search probes inflaton-potential heights $V^{1/4} \gtrsim 4 \times 10^{15}$ GeV, then CS-induced shear does not constitute a background. In this case, one strategy is to integrate deeply on $\sim 5^\circ \times 5^\circ$ patch of sky with moderate ($\sim 0.5^\circ$) resolution.

For a one-year experiment with NET $s \geq 10\mu\text{K}\sqrt{\text{sec}}$ (e.g., Planck, BICEP, QUIET), this is the best strategy. However, if the large-angle temperature-polarization cross-correlation is as large as WMAP indicates, then there will be a large reionization bump in the curl power spectrum. If so, then a similar sensitivity to gravitational waves might be achievable with a full-sky map with $\sim 0.5^\circ$ angular resolution and similar detector sensitivity.

However, if the effective detector sensitivity is $s \lesssim 10\mu\text{K}\sqrt{\text{s}}$, then inflaton-potential heights $V^{1/4} \lesssim 4 \times 10^{15}$ GeV can be probed. For these smaller-amplitude gravitational-wave signals, the CS-induced shear will be a foreground for the $l \sim 50 - 100$ GW-induced C_l^{CC} . This foreground must be removed with higher-order correlations, which requires a full-sky map of the temperature and polarization with $\theta_{\text{fwhm}} \sim \text{arcmins}$. This will have to be the route for post-Planck $s \sim 1\mu\text{K}\sqrt{\text{sec}}$ experiment such as CMBPOL. With quadratic estimators, the lowest detectable inflaton-potential height V is $V^{1/4} \sim 10^{15}$ GeV [23,24], although one may be able to do a bit better with higher-order estimators [29,30]. Anything smaller will be lost in the CS-induced curl, even after subtraction with higher-order correlations. However, with a large-angle reionization bump, as suggested by recent WMAP measurements, the gravitational-wave signal at large angles may be as easily detectable as the smaller-angle signal, without being confused by the CS-induced curl [31]. The “best” survey strategy is still not entirely clear, and will depend on experimental factors as well as these more theoretical considerations. These questions are the subject of several ongoing NASA mission concept studies.

10. Closing Comments

In these lectures, we have provided details of some of the theory of CMB polarization. The reader who has successfully gone through all of the Exercises may take pride in the knowledge that he/she has achieved a mastery of the technical aspects of the subject comparable to that of many researchers in the field. Of course, these lectures still leave many essential aspects of CMB polarization theory uncovered. These include techniques for solving the Boltzmann equations and a more intuitive understanding of the features of the power spectra. The reader should also be aware that the full- or flat-sky tensor-harmonic formalism must necessarily be altered to analyze real CMB maps. Such maps will have sky cuts and so the measured regions of sky will be less than the full sky and may be irregularly shaped. Sophisticated techniques for dealing with a cut sky have now been developed, and many other issues that accompany analysis of real maps are highly nontrivial and completely neglected here.

The past few years have been quite exciting for the CMB. There is also clearly a very active foreseeable future in the field with a number of targets for experimentalists: e.g., the polarization autocorrelation function, detection of weak-lensing, and the longer-term goal of detecting inflationary gravitational-wave background. If the past is any guide, however, chances are that the most exciting discoveries are those that theorists have not yet anticipated.

Appendix: Rotational invariance of an ‘spin-2 field’

Here we demonstrate the rotational invariance of Eq. (14). Let us begin by considering the usual rotational matrix,

$$x'_k = A^j_k x_j. \quad (140)$$

The derivative operator transforms as

$$\frac{\partial F}{\partial x_j} = \frac{\partial F}{\partial x'_i} \frac{\partial x'_i}{\partial x_j}. \quad (141)$$

From Eq. (140), we obtain

$$\frac{\partial x'_i}{\partial x_j} = \frac{\partial}{\partial x_j} (A^s_i x_s) = A^s_i \frac{\partial x_s}{\partial x_j} = A^j_i, \quad (142)$$

and Eq. (141) becomes

$$\frac{\partial F}{\partial x_j} = \frac{\partial F}{\partial x'_i} A^j_i. \quad (143)$$

Thus, the derivative operator in the rotated system transforms as

$$\frac{\partial}{\partial x'_i} = (A^{-1})^k_i \frac{\partial}{\partial x_k}. \quad (144)$$

Taking into account Eq. (8), Eq. (14) becomes

$$\partial'_i \partial'_j P'_{ij} = (A^{-1})^k_i \partial_k (A^{-1})^l_j \partial_l A^i_m A^j_n P_{mn} = \delta^l_n \delta^k_m \partial_k \partial_l P_{mn} = \partial_k \partial_l P_{kl}. \quad (145)$$

Acknowledgments

MK was supported in part by NASA NAG5-11985, and DoE DE-FG03-92-ER40701. We thank the organizers of the Villa Mondragone School of Gravitation and Cosmology for inviting these lectures and for their hospitality. We also thank J. Pritchard, M. Doran, A. Cooray, A. Kosowsky, and K. Sigurdson for comments on an earlier draft.

References

1. P. de Bernardis et al., *Nature (London)* 404, 955 (2000); A. D. Miller et al., *Astrophys. J. Lett.* 524, L1 (1999); S. Hanany et al., *Astrophys. J. Lett.* 545, L5 (2000); N. W. Halverson et al., *Astrophys. J.* 568, 38 (2002); B. S. Mason et al., *Astrophys. J.* 591, 540 (2003); A. Benoit et al., *Astron. Astrophys.* 399, L2 (2003); J. H. Goldstein et al., *Astrophys. J.* 599, 773 (2003); D. N. Spergel et al., *Astrophys. J. Suppl.* 148, 213 (2003).
2. E. M. Leitch et al., *Nature* 420, 763 (2002); A. Kogut et al., *Astrophys. J. Suppl.* 148, 161 (2003).
3. See, e.g., M. Kamionkowski and A. Kosowsky, *Ann. Rev. Nucl. Part. Sci.* 49, 77 (1999); W. Hu and S. Dodelson, *Ann. Rev. Astron. Astrophys.* 40, 171 (2002). M. White and J. D. Cohn, astro-ph/0203120 provides a very comprehensive review of the literature.

4. S. Dodelson, *Modern Cosmology* (Academic Press, 2003); A. Liddle and D. H. Lyth, *Cosmological Inflation and Large-Scale Structure* (Cambridge University Press, 2000).
5. M. J. Rees, *Astrophys. J. Lett.* 153, 1 (1968); A. Kosowsky, *Ann. Phys.* 246, 49 (1999).
6. See., e.g., J. D. Jackson, *Classical Electrodynamics* (John Wiley and Sons, 1998); G. B. Rybicki and A. P. Lightman, *Radiative Processes in Astrophysics* (John Wiley and Sons, 1979).
7. A. Kosowsky, *New Astron. Rev.* 43, 159 (1999).
8. A. Cooray, A. Melchiorri, and J. Silk, *Phys. Lett. B* 554, 1 (2003).
9. S. Chandrasekhar, *Radiation Transfer* (Dover, 1960).
10. M. Kamionkowski, A. Babul, C. M. Cress, and A. Refregier, *MNRAS* 301, 1064 (1998); A. Stebbins, astro-ph/9609149.
11. M. Kamionkowski, A. Kosowsky, and A. Stebbins, *Phys. Rev D* 55, 7368 (1997); *Phys. Rev. Lett.* 78, 2058 (1997).
12. M. Zaldarriaga and U. Seljak, *Phys. Rev. D* 55, 1830 (1997); U. Seljak and M. Zaldarriaga, *Phys. Rev. Lett.* 78, 2054 (1997).
13. W. Hu and M. White, *Phys. Rev. D* 56, 596 (1997).
14. A. G. Polnarev, *Sov. Astron.* 29, 607 (1985); see also R. G. Crittenden, PhD thesis, University of Pennsylvania (1993).
15. P. J. E. Peebles *The Large-Scale Structure of the Universe* (Princeton University Press, 1980).
16. R. R. Caldwell, M. Kamionkowski, and L. Wadley, *Phys. Rev. D* 59, 027101 (1999).
17. C.-P. Ma and E. Bertschinger, *Astrophys. J.* 455, 7 (1995).
18. A. Lue, L. Wang, and M. Kamionkowski, *Phys. Rev. Lett.* 83, 1506 (1999). N. Lepora, gr-qc/9812077.
19. M. Zaldarriaga and D. Harari, *Phys. Rev. D* 52, 3276 (1995).
20. K. L. Ng and K.-W. Ng, *Astrophys. J.* 456, 413 (1996); M. Zaldarriaga, *Phys. Rev. D* 55, 1822 (1997).
21. A. Jaffe, M. Kamionkowski, and L. Wang, *Phys. Rev. D* 61, 083501 (2000).
22. M. Zaldarriaga and U. Seljak, *Phys. Rev D* 58, 023003 (1998).
23. M. Kesden, A. Cooray, and M. Kamionkowski, *Phys. Rev Lett.* 89, 011304 (2003).
24. L. Knox and Y.-S. Song, *Phys. Rev Lett.* 89, 011303 (2003).
25. A. Lewis, A. Challinor, and N. Turok, *Phys. Rev. D* 65, 023505.
26. U. Seljak and M. Zaldarriaga, *Phys. Rev. Lett.* 82, 2636 (1999).
27. W. Hu and T. Okamoto, *Astrophys. J.* 574, 566 (2002).
28. M. Kesden, A. Cooray, and M. Kamionkowski, *Phys. Rev. D* 67, 123507 (2003).
29. C. M. Hirata and U. Seljak, *Phys. Rev. D* 68, 083002 (2003); U. Seljak and C. M. Hirata, astro-ph/0310163.
30. A. Amblard, C. Vale, and M. White, astro-ph/0403075.
31. W. Hu, talk at Kavli-CERCA Conference on the Future of Cosmology, Oct 10–12, 2003, Cleveland, Ohio.